Bulletin of the Seismological Society of America, Vol. 100, No. 6, pp. 2873–2890, December 2010, doi: 10.1785/0120090377

# Geological and Seismological Analysis of the 13 February 2001 $M_w$ 6.6 El Salvador Earthquake: Evidence for Surface Rupture and Implications for Seismic Hazard

by Carolina Canora, José J. Martínez-Díaz, Pilar Villamor, Kelvin Berryman, José A. Álvarez-Gómez, Carlos Pullinger, and Ramón Capote

**Abstract** The El Salvador earthquake of 13 February 2001 ($M_w$ 6.6) caused tectonic rupture on the El Salvador fault zone (ESFZ). Right-lateral strike-slip surface rupture of the east–west trending fault zone had a maximum surface displacement of 0.60 m. No vertical component was observed. The earthquake resulted in widespread landslides in the epicentral area, where bedrock is composed of volcanic sediments, tephra, and weak ignimbrites. In the aftermath of the earthquake, widespread damage to houses and roads and the hazards posed by landslides captured the attention of responding agencies and scientists, and the presence of surface-fault rupture was overlooked. Additionally, the tectonic context in which the earthquake took place had not been clear until mapping of the ESFZ was completed for the present study. We identified several fault segments, the distribution of surface ruptures, the aftershock pattern, and fault-rupture scaling considerations that indicate the 21-km-long San Vicente segment ruptured in the 2001 event. Static Coulomb stress transfer models for the San Vicente rupture are consistent with both aftershock activity of the 2001 sequence and ongoing background seismicity in the region. At $M_w$ 6.6, the 2001 earthquake was of only moderate magnitude, yet there was significant damage to the country's infrastructure, including buildings and roads, and numerous deaths and injuries. Thus, earthquake hazard and risk in the vicinity of the ESFZ, which straddles the city of San Salvador with a population of $>2$ million, is high because even moderate-magnitude events can result in major damage, deaths, and injuries in the region.

## Introduction

On 13 February 2001, an $M_w$ 6.6 earthquake struck the central region of El Salvador (Central America) at a hypocentral depth of $10 \pm 5$ km. An earlier, large normal-faulting event ($M_w$ 7.7, hypocentral depth of 54 km) occurred within the subducting Cocos plate 40 km off the Salvadorian coast only one month earlier (13 January 2001). Although the 13 February event was smaller in magnitude than the January earthquake, the February earthquake was shallower and near major urban areas and, as a result, caused substantial damage. The January $M_w$ 7.7 subduction-related earthquake resulted in more than 900 deaths and severe damage (mainly caused by large earthquake-induced landslides). The February $M_w$ 6.6 earthquake caused more than 300 deaths and more large landslides. Because the widespread damaging landslides triggered by the February $M_w$ 6.6 earthquake and immediate focus on the emergency response, no geological investigations were undertaken to identify the tectonic structure responsible for this event. Most of the scientific response concentrated on the study of mass movements triggered by seismic shaking.

Destructive earthquakes similar to the 2001 events have occurred during the last century in El Salvador (Bommer *et al.*, 2002), as is expected at a plate boundary where the relative motion between the plates is 70–85 mm/yr (DeMets, 2001) (Fig. 1). El Salvador deformation associated with trench-parallel strike-slip movement in the upper crust is estimated to be at least 8 mm/yr (DeMets *et al.*, 2008). It is possible that earlier historic earthquakes had surface rupture, but, prior to this study, the distribution of active faults in El Salvador has only been known in the most general way (Martínez-Díaz *et al.*, 2004; Corti *et al.*, 2005).

In this paper, we present field evidence of surface rupture associated with the 13 February 2001, $M_w$ 6.6 earthquake, define the seismic source, and infer the fault rupture area from seismic and geological data. We also present the first detailed active fault map of the area where the earthquake

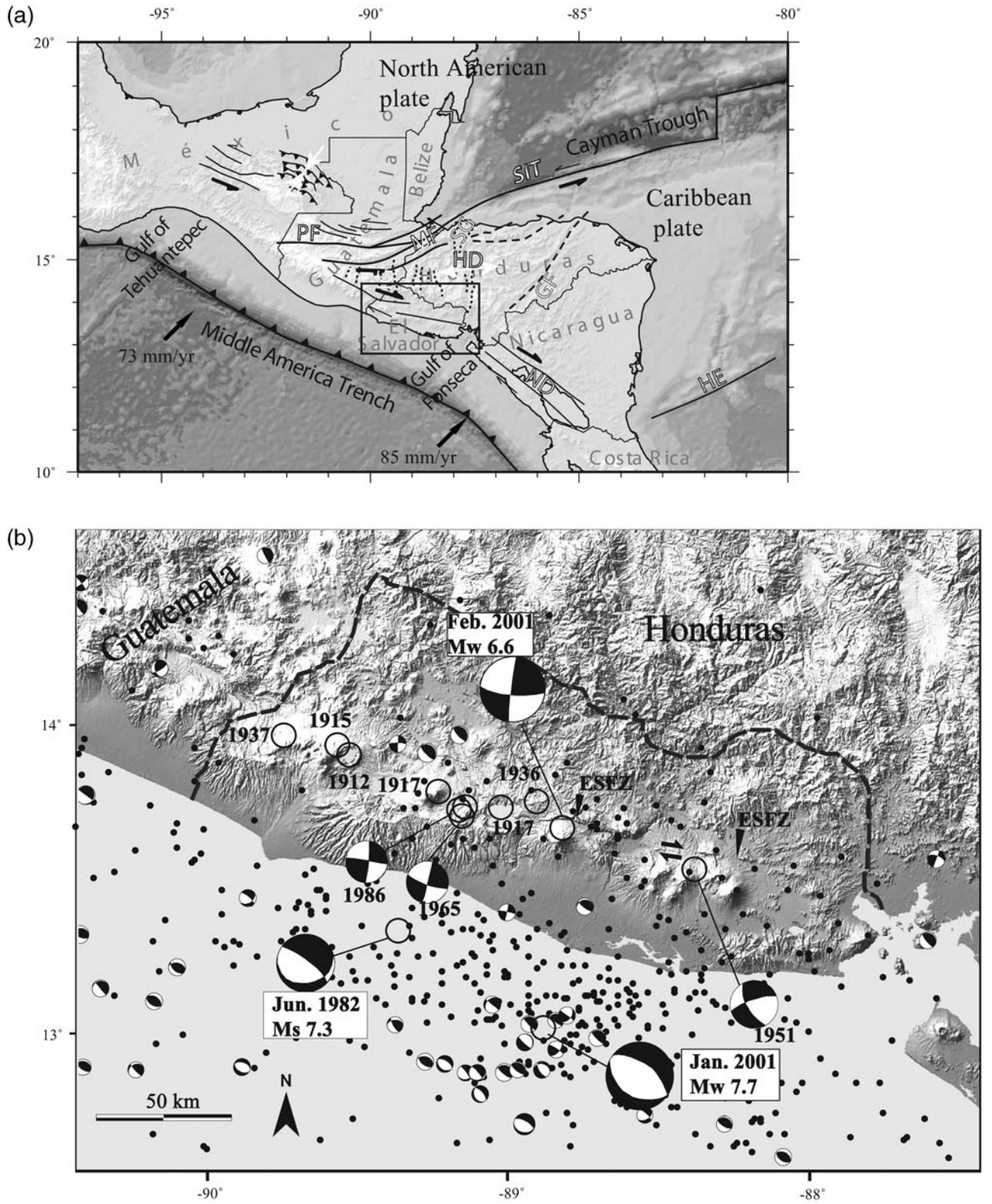


**Figure 1.** Tectonic setting of northern Central America. (a) Tectonic plates, major crustal blocks, and faults. Arrows show relative directions of displacements. PF, Polochic fault; MF, Motagua fault; SIT, Swan Island transform; SG, Sula graben; IG, Ipala graben; HD, Honduras depression; GF, Guayape fault; ND, Nicaraguan depression; HE, Hess escarpment. (b) Shuttle Radar Topography Mission (SRTM) image of El Salvador with historically destructive earthquakes (black circles) and instrumental epicenters (small dots) ($M_s > 2.5$, period 1977–2001) from the USGS–National Earthquake Information Center (NEIC) catalogue (see Data and Resources section). Small focal-mechanism symbols are for events of $M_w > 5.5$ (1977–2001, Global CMT database; see Data and Resources section), and large focal-mechanism symbols are for events of $M_w > 6.5$ (from Buforn *et al.*, 2001). ESZF, El Salvador fault zone; black dashed line, El Salvador border.

occurred. The study involved spatial and temporal analysis of the seismic sequence and its relation to surface-rupture features; review of vertical aerial photograph and analysis of digital terrain models (DTM) to map active faults in the earthquake area; and field reconnaissance of the possible surface rupture and secondary effects associated with the earthquake along mapped fault traces. Spatial analysis of landslides triggered by the earthquake also helped us to define the probable length of surface-fault rupture.

We calculated Coulomb static stress changes for the geologically defined fault rupture model associated with the 13 February 2001 mainshock. We did this to evaluate the coherence of our rupture model with the spatial and temporal distribution of aftershocks. Coulomb static stress analysis also helped us determine the stress loading produced by the 2001 sequence on active faults in the area, which has important implications for the local seismic hazard.

## Geological and Seismotectonic Setting

Central El Salvador is located in the northern part of the Central America volcanic arc that extends from Guatemala to Costa Rica along the active Pacific margin (Fig. 1a). This volcanic arc is associated with the subduction of the Cocos plate beneath the Caribbean plate. The arc ends abruptly to the north against the Polochic fault in Guatemala, in a diffuse triple junction between the Cocos, Caribbean, and North American plates (Plafker, 1976; Guzmán-Speziale *et al.*, 1989; Guzmán-Speziale and Meneses-Rocha, 2000; Lyon-Caen *et al.*, 2006).

The Cocos plate converges with the Caribbean plate at 70–85 mm/yr and has a small oblique component (DeMets, 2001). The forearc sliver between the Mesoamerican trough and the Central American volcanic arc is moving northwest relative to the Cocos plate, parallel to the trough. DeMets (2001) considered this displacement to be the result of strain partitioning, which produces a strike-slip regime along the volcanic arc and explains the strike-slip focal mechanisms of larger earthquakes in this area. However, recent Global Positioning System velocity data show that the degree of coupling in this part of Central America is very low (Correa-Mora *et al.*, 2009), suggesting that strain partitioning may not be an effective driving mechanism and that the strike-slip regime along the volcanic arc is actually driven by the relative eastward drift of the Caribban plate (Álvarez-Gómez *et al.*, 2008).

The Salvadorian sector of the subduction zone contains two distinct zones that have contrasting earthquake focal mechanisms: thrusting along the Wadati–Benioff zone and normal faulting within the subducting plate from extensional forces generated by slab-pull forces or bending of the subducting plate (Isacks and Baranzagi, 1977). The largest earthquakes ($M_w > 7.0$) along the subducting plate tend to rupture at intermediate depths and can cause moderately intense shaking across wide parts of southern El Salvador. The most recent example of such an event is the 13 January 2001 $M_w$ 7.7 earthquake (Bommer *et al.*, 2002) that produced several catastrophic landslides in El Salvador (Baum *et al.*, 2001; Jibson and Crone, 2001). Other large earthquakes in this section of the subduction zone (in 1921, 1932, and 1982) have almost identical normal-slip mechanisms to the January 2001 event, with the principal plane oriented N120°/130° E.

The El Salvador region is characterized by high seismic activity in the upper overriding plate (Fig. 1b). Shallow (< 20 km depth) crustal events occur along the chain of Quaternary volcanoes (e.g., Dewey *et al.*, 2004) and accommodate trench-parallel strike-slip motion (White *et al.*, 1987). Historically their magnitudes are smaller than the large subduction earthquakes and range between $M_w$ 5.5 and $M_w$ 6.8. The 13 February 2001 $M_w$ 6.6 event is representative of these larger upper plate earthquakes (Bommer *et al.*, 2002). Despite their small to moderate magnitudes, upper crustal earthquakes have produced greater destruction in El Salvador than the less frequent large magnitude earthquakes in the subduction zone (White and Harlow, 1993) mainly because of their short recurrence intervals, shallow depths, and proximity to population centers.

The 11 destructive shallow crustal earthquakes that have occurred in El Salvador during the twentieth century are aligned along the volcanic arc (Fig. 1b). On 8 June 1917, an $M_s$ 6.4 earthquake occurred 30–40 km east of the San Salvador volcano, followed by an $M_s$ 6.3 earthquake. On 28 April 1919 San Salvador was again shaken by a shallow $M_s$ 5.9 earthquake situated at about the same location of the 1986 $M_w$ 5.7 earthquake that originated in the volcanic arc and propagated along a nearly vertical, north-to-northeast striking plane (White *et al.*, 1987). Four reliable focal mechanisms are available for the more recent major events of 1951, 1965, 1986, and February 2001 (Martínez-Díaz *et al.*, 2004, and references therein). They are all strike-slip events with one of the nodal planes oriented east–west, parallel to the volcanic arc.

## February 2001 Seismic Sequence

The epicenter of the 13 February 2001 El Salvador $M_w$ 6.6 earthquake was located near the city of San Vicente (13.621° N, 88.856° W), 30 km east of San Salvador (Ministerio de Medio Ambiente y Recursos Naturales–Servicio Nacional de Estudios Territoriales [MARN–SNET] local network; see Data and Resources section). The mainshock was followed by aftershocks that covered an area of 300 km$^2$ (Fig. 2 and Fig. 3a). The total source time function duration was 12 s (Bommer *et al.*, 2002). The focal depth was 9 km (from the MARN–SNET local network), and the focal mechanism is resolved as a left-lateral motion on a N7°E-striking plane or a right-lateral motion on a N96°E-striking plane. Previous studies of the aftershock distribution concluded that the N96°E-striking plane with right-lateral motion is the more likely orientation of the fault that ruptured in the earthquake (Bommer *et al.*, 2002; Martínez-Díaz *et al.*, 2004).

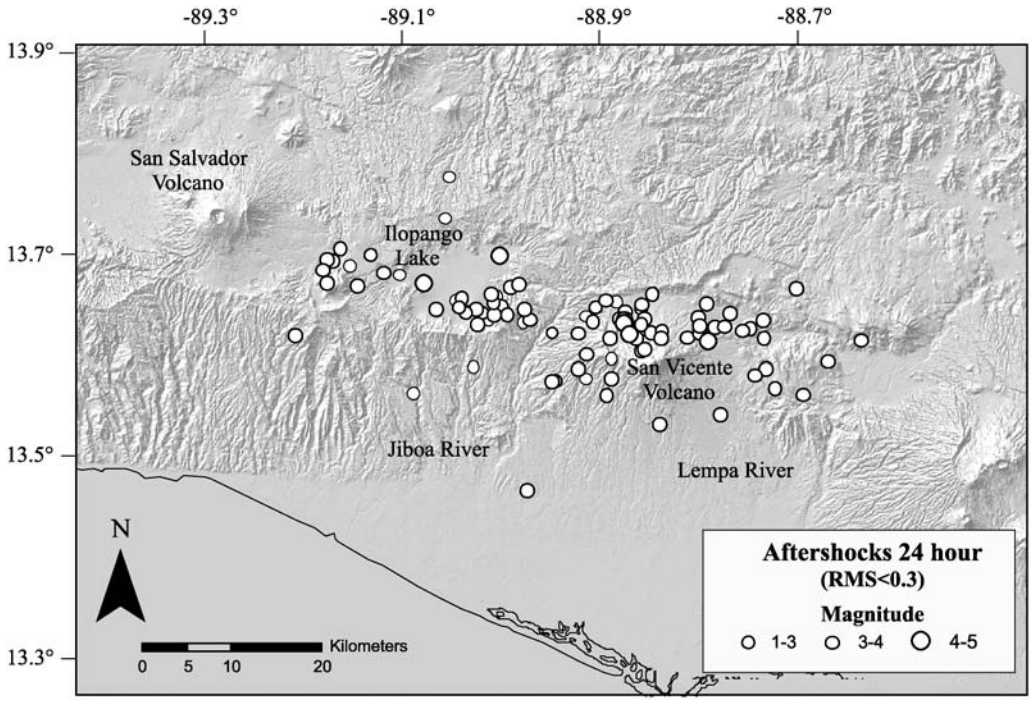


**Figure 2.** Aftershock distribution for events within 24 hours after the 13 February 2001 mainshock.

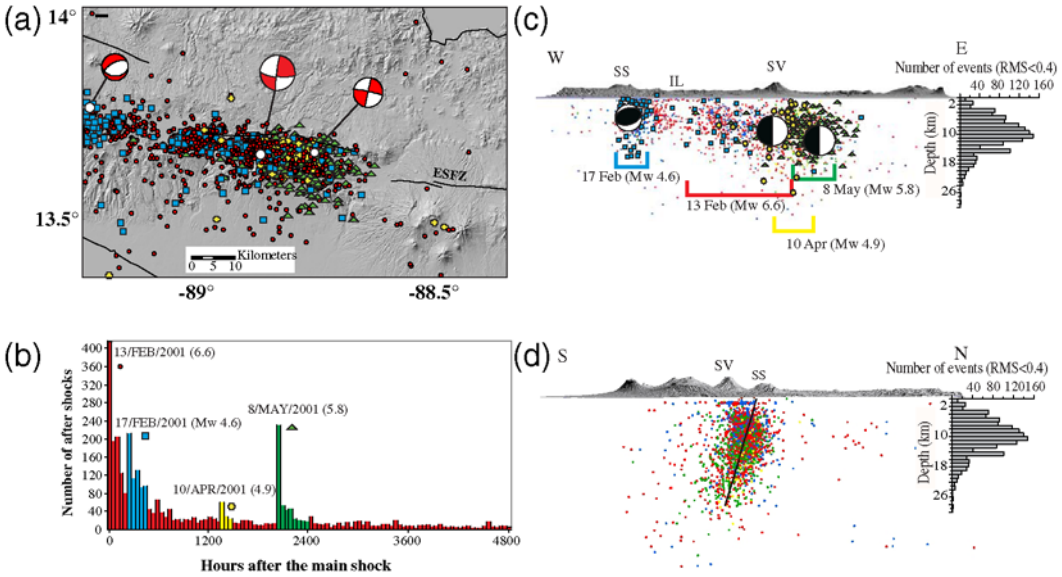


**Figure 3.** (a) Seismicity of the region of the El Salvador fault zone for six months following the 13 February 2001 mainshock. Hypocenters and epicenters are from the Servicio Nacional de Estudios Territoriales (SNET) catalog (Buforn *et al.*, 2001) and focal mechanisms are from the Global Centroid Moment Tensor (CMT) and USGS–NEIC catalogs (see Data and Resources section). The principal aftershocks are represented with three different symbol types (squares, $M_w$ 4.6 on 17 February ; crosses, $M_w$ 4.9 on 10 April; triangles, $M_w$ 5.8 on 8 May), while the aftershocks related to the mainshock are circles. (b) The number of events as a function of time for the period 13 February–31 May 2001, identified by those symbols associated with the 13 February mainshock and principal aftershocks (as in part a). (c and d) Seismicity cross sections of the 2001 earthquake sequence parallel and perpendicular to the fault, respectively. We show a fault plane that is the best fit with the aftershock seismicity. SS, San Salvador volcano; SV, San Vicente volcano; and IL, Ilopango Lake. The color version of this figure is available only in the electronic edition.

### Spatial and Temporal Analysis of the Aftershock Sequence

The aftershocks associated with 13 February 2001 event help determine the geometry and size of the coseismic rupture plane and the geometry of the fault that generated the earthquake. The distribution of the aftershocks for 24 hours following the mainshock covers an area that is 60 km long, and 20 km wide (Fig. 2), an area that we interpret to be longer than the rupture plane. For most large mainshocks, aftershocks occur near both terminations of the rupture (Das and Henry, 2003) due to dynamic stress increase (Das and Scholz, 1981). Geological and morphological observations lead us to consider the primary rupture plane for the 13 February 2001 El Salvador earthquake was about 21 km long.

Figure 3 shows the distribution of the aftershocks relocated by MARN–SNET with local observations for a period of six months after the mainshock. This distribution helps define the geometry of the fault in the rupture area. In this figure, we show the epicenter locations of three large aftershocks (17 February $M_w$ 4.6 event, the 10 April $M_w$ 4.9 event, and the 8 May $M_w$ 5.8 event) and clusters of the smaller events in the aftershock sequence. The 17 February aftershock produced significant damage in San Salvador (Bommer *et al.*, 2002). This aftershock has a normal faulting mechanism associated with the reactivation of northeast–southwest normal faults on the flank of San Salvador volcano.

The spatial distribution of aftershocks extends for at least 60 km along an east–west trend in the area of the mainshock and along an approximately N105° E trend around the 8 May $M_w$ 5.8 aftershock area (subparallel to the volcanic chain). The aftershock zone has a width of about 10 km, and 95% of the events are ≤15 km deep. Thus, it appears that the fault may change orientation at the eastern end of the aftershock area. The three-dimensional spatial aftershock distribution (Fig. 3c,d) suggests a fault plane that dips 70°–85° S.

Because the spatial distribution of 6 months of aftershocks represents a larger area than the fault rupture area itself, we compared it with the distribution of the energy released during the mainshock and during the first 24 hours of aftershocks (Fig. 4a,b). We computed maps of seismic moment using the formulation of Kanamori (1977) for each event in cells having an area of 0.02 × 0.02 decimal degrees for each of the time intervals. Representing the earthquake sequence in terms of energy release is a more effective way of visualizing fault kinematics than simply showing epicenters (Selvaggi *et al.*, 1997).

Figure 4a shows the energy release in the mainshock based on the model of slip distribution by Kikuchi and Yamanaka (2001). The coseismic slip on the plane is irregular and, starting with a maximum of 3 m in the western part of the rupture, diminishes eastward and upward. Figure 4b shows the total energy released in the first 24 hours of the aftershock sequence. The energy release following the mainshock is larger to the east of the mainshock rupture and is generally more concentrated in the east than in the west. The distribution of aftershocks fits well with the fault-mechanics model of Scholz (1994), which predicts a lower density of close-to-fault aftershocks adjacent to the mainshock slip patches (with the highest stress drop), and more frequent aftershocks releasing energy where mainshock slip was lower. The Kikuchi and Yamanaka (2001) rupture model suggests about 0.5 m of surface rupture and an approximate surface rupture length of 24 km.

### Active Faults in the February 2001 Earthquake Area: The El Salvador Fault Zone

In this study, we expanded on the recent mapping of Benito *et al.* (2004), Martínez-Díaz *et al.* (2004), Corti *et al.* (2005), and Agostini *et al.* (2006) and have identified a major fault, the El Salvador fault zone (ESFZ), in the vicinity of the 2001 earthquake sequence. This fault had not been described at the time of the 2001 earthquake, and postearthquake studies primarily focused on major coseismic landslides. We present new mapping in which we identified fault traces that ruptured in the 2001 earthquake sequence, define their geometry, and, based on these data, reevaluate fault segmentation.

Our regional fault mapping covers an area larger than the 2001 earthquake sequence (Fig. 5); and our detailed mapping focused on the area of the 2001 earthquake sequence (Fig. 6). We analyzed a DTM (with 10-m pixel resolution), examined aerial photographs, and conducted ground investigations.

Based on fault geometry, the distribution of seismicity associated with the 2001 sequence, the morphology of the fault zone, and the segmentation proposed by other authors (Corti *et al.*, 2005; Agostini *et al.*, 2006), we propose four segments for the ESFZ, extending from Ilopango Lake to the Gulf of Fonseca (Fig. 5); from west to east they are the San Vicente, Lempa, Berlin, and San Miguel segments. We mapped the San Vicente and Lempa segments in detail (Fig. 6).

There are marked differences in the patterns of fault traces between the four segments. The San Vicente and Berlin segments have simple, clear east–west strike-slip principal displacement zones and some secondary northwest–southeast faulting. The approximately 21-km-long San Vicente segment extends from the Ilopango Caldera to the city of San Vicente. The Berlin segment extends for about 24 km from the Lempa River to Berlin Volcano. From San Vicente to Lempa River, the Lempa segment consist of fault strands where the strike-slip deformation is distributed in a 15-km-wide band. Within this area, the zone contains three fault sets: north-northwest–south-southeast and northwest–southeast normal faults that have a horizontal slip component, and east–west strike-slip faults (Fig. 6). In this segment, some ends of normal faults are rotated by drag-folding associated with approximately east–west strike-slip movement. The easternmost segment, the San Miguel segment, extends for about 50 km from San Miguel Volcano

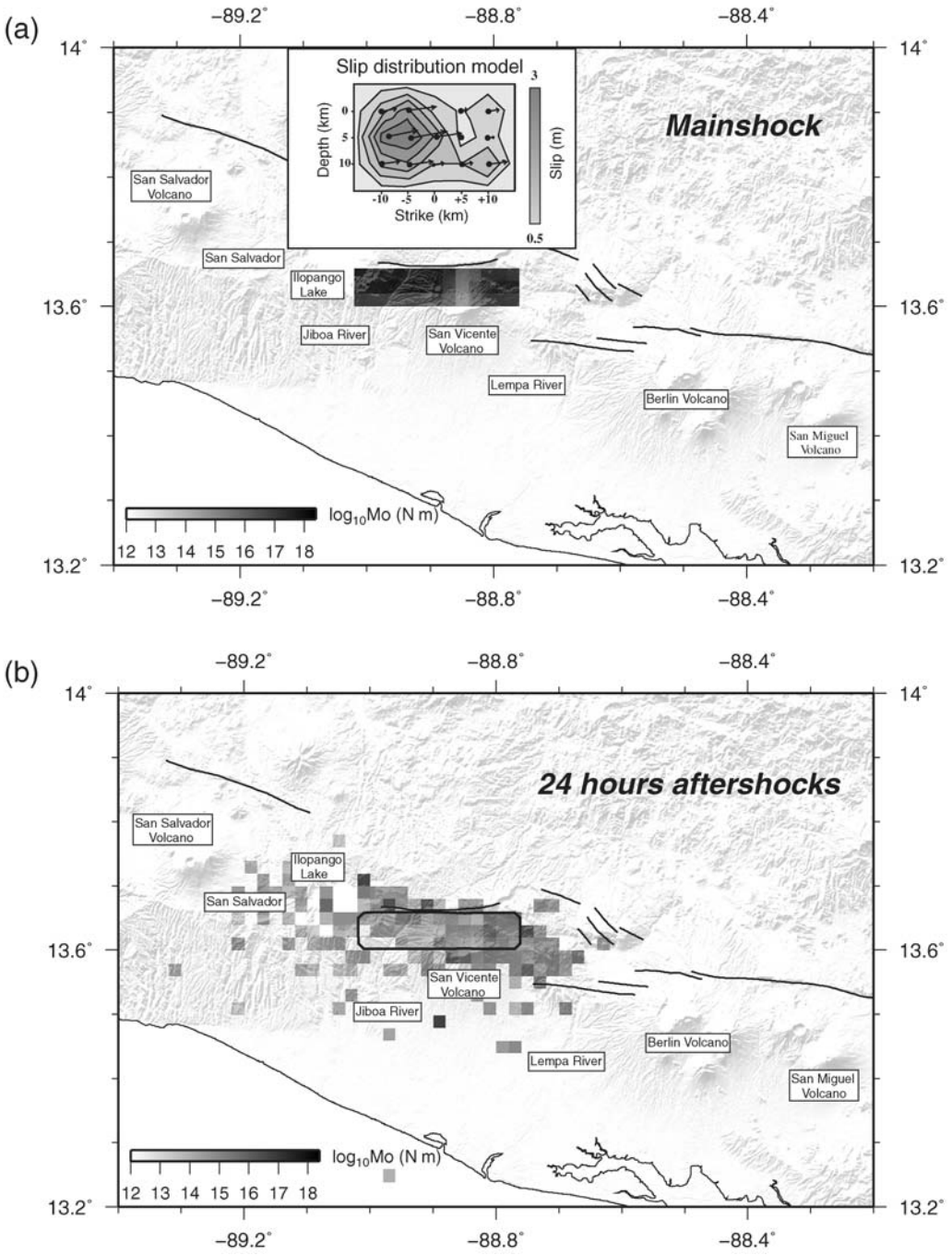


**Figure 4.** (a) Map of the total energy released in the 13 February 2001 El Salvador mainshock based on the finite-fault slip model of Kikuchi and Yamanaka (2001) (inset). (b) Distribution of energy released in aftershocks during the 24 hours following the mainshock. Darker color shows larger energy release.

to the Gulf of Fonseca and comprises many short fault traces arranged in a right-lateral en echelon array with no clear principal displacement zone. The morphology, structure, and seismicity associated with this segment is consistent with early-stage development of a strike-slip fault zone (Sylvester, 1988).

West of San Salvador, the ESFZ is not clear in terms of fault geometry and morphology, but we infer the existence of another fault segment on the basis of strike-slip fault mechanisms of several large earthquakes with east–west and north–south fault planes (Fig. 1b; Martínez-Díaz *et al.*, 2004).

## On-Fault and Off-Fault Coseismic Surface Deformation Analysis

One main objective of this study is to determine whether the 13 February 2001 earthquake was associated with surface

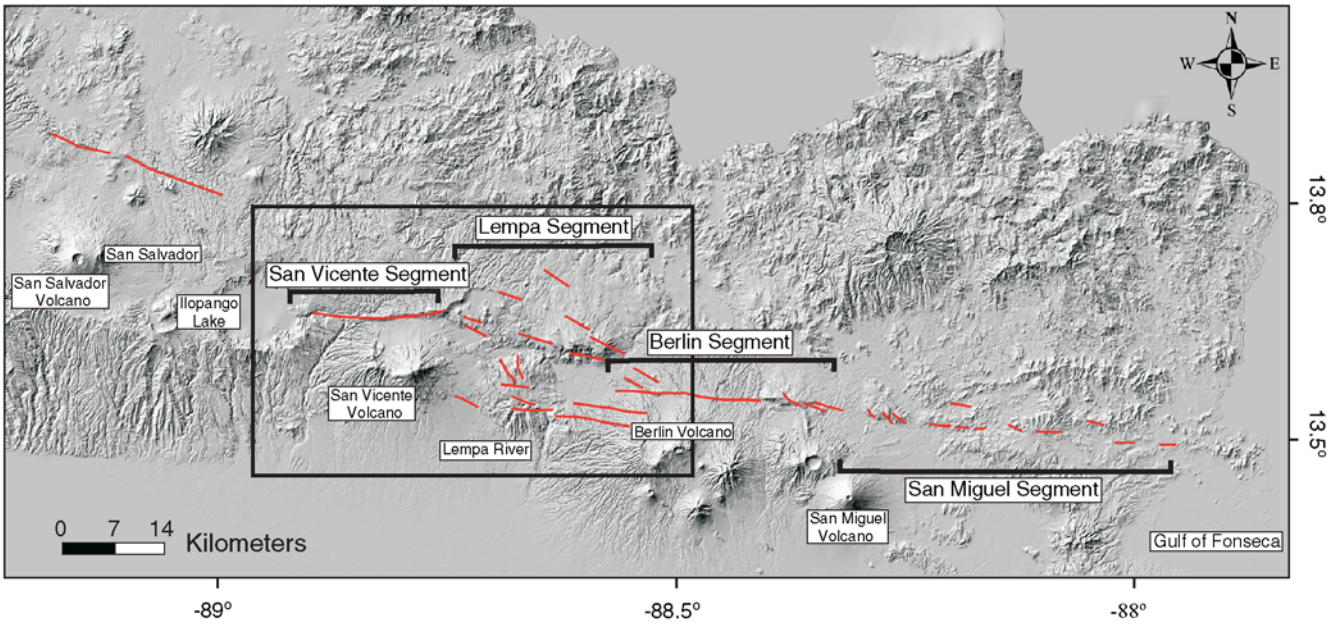


**Figure 5.** Digital terrain model (DTM) of west–central El Salvador with the active fault strands and segments related to the El Salvador fault zone. Area enclosed in rectangle is shown in Figure 6. The color version of this figure is available only in the electronic edition.

rupture of any mapped fault traces of the ESFZ. For that purpose, we compiled information on possible on-fault and off-fault coseismic ground deformation associated with the earthquake, including review of aerial and ground photographs taken a few hours after the earthquake and extensive fieldwork (2005–2008). We obtained detailed photos of

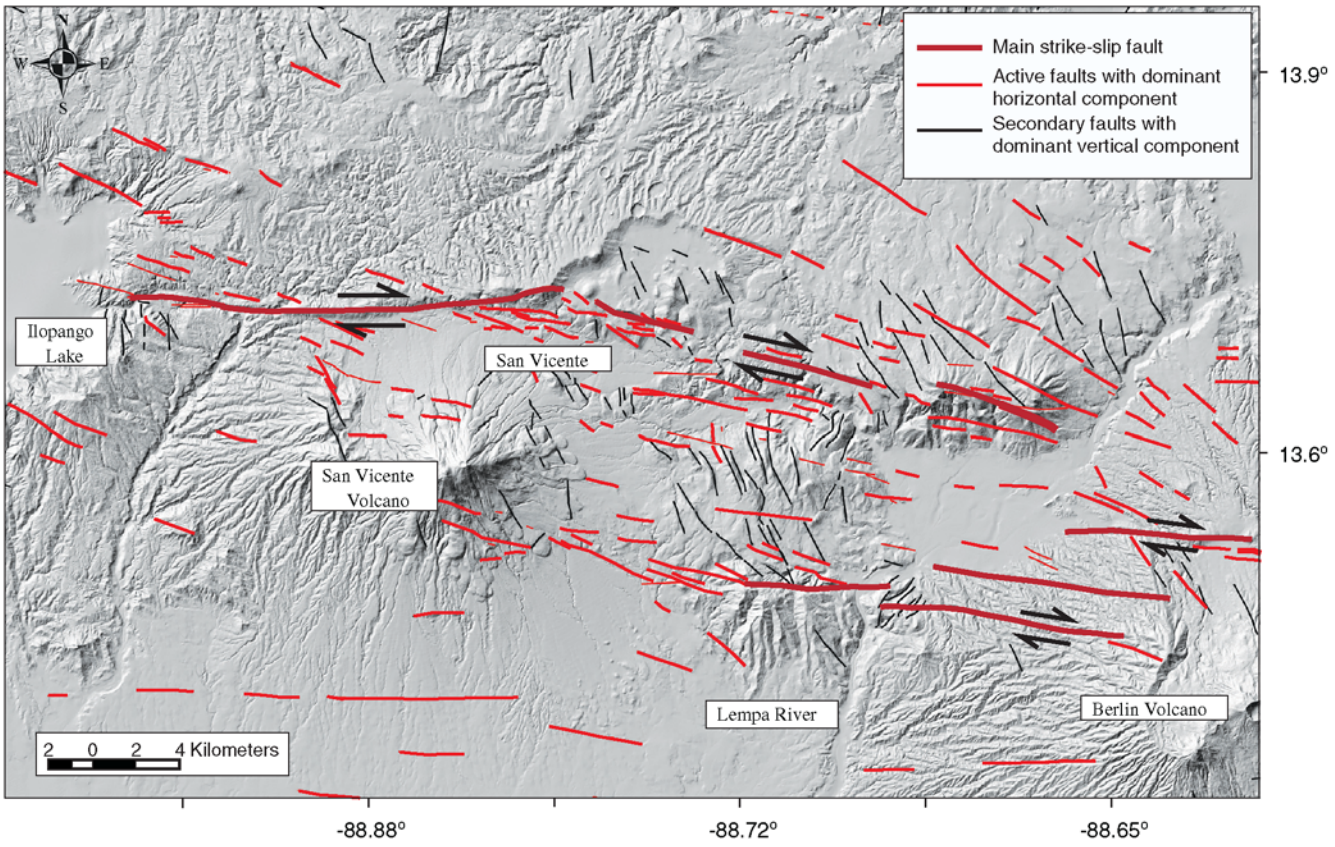


**Figure 6.** Active traces of the San Vicente and Lempa fault segments mapped in this study. The color version of this figure is available only in the electronic edition.

damaged roads and urban areas and of abundant landslides, along with reports from the emergency response team that compiled information from several sources (internal reports from SNET; Manuel Díaz, personal comm. 2008). We then visited sites with possible surface-fault rupture and conducted detailed mapping of the features along the San Vicente and Lempa segments of the fault (Fig. 7). During this field work, we also interviewed several eyewitnesses.

We described the coseismic ground-deformation features as "on-fault" and "off-fault" to distinguish between those directly related to possible surface rupture and those related to earthquake-triggered deformation away from the fault. Eyewitness accounts, together with the photos taken shortly after the earthquake, have been of great help in determining the time of formation of certain features (i.e., whether they were coseismic or not). In this study, we only include those features that have been useful in assessing fault location and rupture associated with the 2001 earthquake.

The on-fault features identified in our study include scarps (with displacement amounts) and fissures (opening cracks and fractures) without displacement that occurred along the mapped active fault traces. These are the expression of primary surface-fault rupture. Off-fault features include cracks and fractures in soils, roads, and buildings related to lateral spreading, landslides, collapse, liquefaction, differential compaction, and subsidence of unconsolidated sediments. There were also hundreds of landslides triggered by the earthquake.

Although none of the features observed and/or photographed after the earthquake have been described as surface-fault rupture prior to this study, our reevaluation of the origin of some features points to the presence of fault surface rupture associated with the 13 February 2001 earthquake. In order to identify the features that we interpret to represent the fault surface rupture, we considered three criteria: (1) if the feature had displacement and it agrees with the rest of the data (e.g., with the focal mechanism); (2) if eyewitnesses say the feature was formed at the time of the earthquake; and, (3) if the feature is located on the fault trace.

### On-Fault Deformation Features

Two surface ruptures located on the El Salvador fault zone (SR1 and SR2 in Figure 7) were associated with the

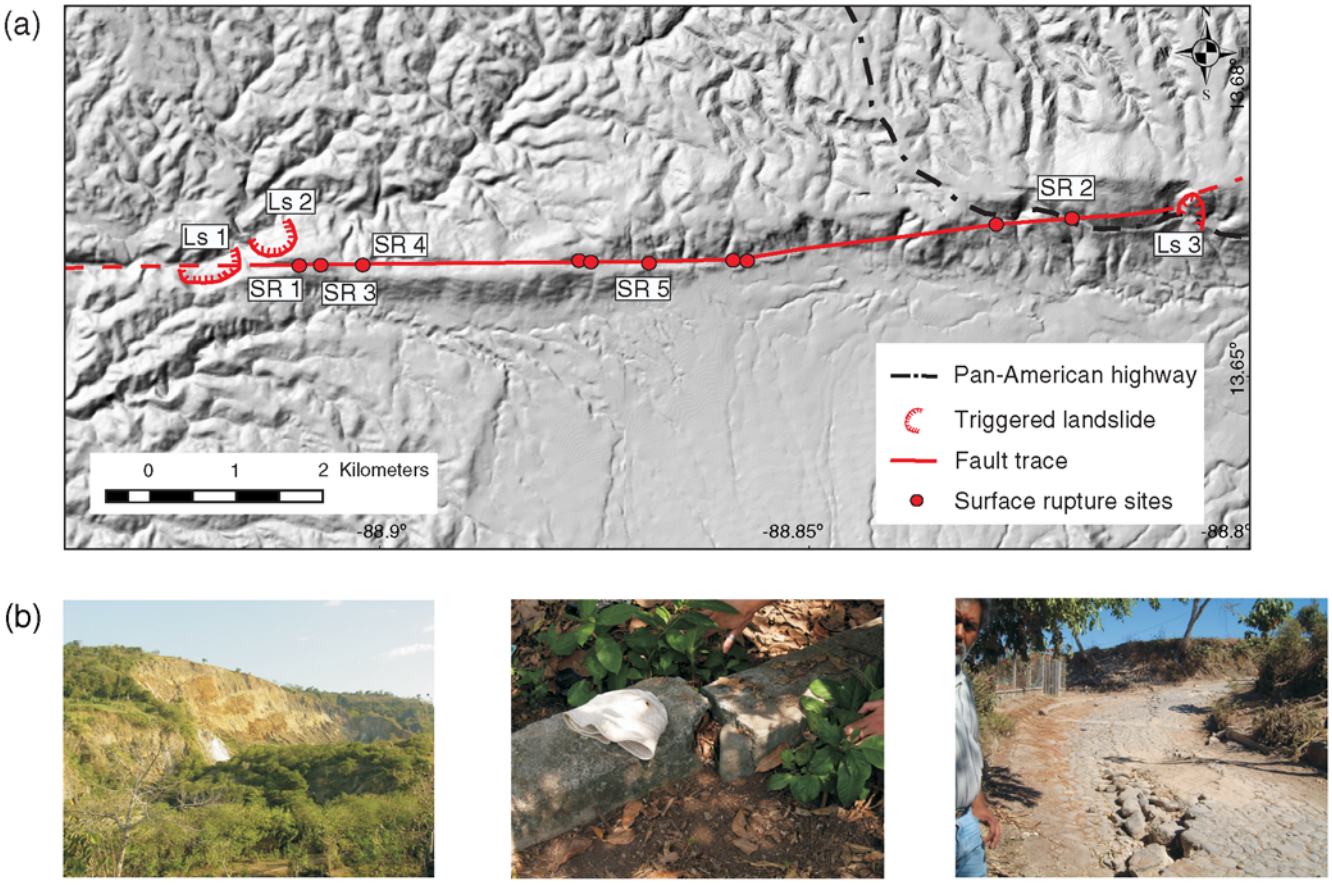


**Figure 7.** (a) Locations along the San Vicente segment where surface rupture and damage associated with the 13 February 2001 earthquake have been documented. Ls1, Ls2, and Ls3 are the main landslides produced by the seismic sequence. SR1-5 are locations where surface rupture has been documented. (b) Photos of three features produced by the earthquake: left, frontal view of the Jiboa landslide triggered by the mainshock (LS1); middle and right, details of surface ruptures along the fault trace. The color version of this figure is available only in the electronic edition.

13 February 2001 El Salvador earthquake. At SR1, we identified two rupture planes with a minimum of 0.6 m of pure right-lateral horizontal offset (Fig. 8). At this point, a N104° E fault clearly displaces the edge of a small road. The other clear surface-rupture (SR2 in Fig. 7) occurred at the Pan-American Highway, 9 km east of SR1. This feature was identified on an aerial photo taken one day after the event, and it was measured at the edge of the highway, where it is still evident today. The minimum coseismic displacement at this point was 0.20 m of pure right-lateral displacement across a 20-m-wide shear structure with en echelon fractures and riedel shears (Fig. 9).

Along the fault, we found three additional possible ruptures related to the 13 February 2001 earthquake (SR3, SR4, and SR5 on Fig. 7). These features are all on the fault trace, and the sense of displacement is consistent with the earthquake; however, there were no eyewitness reports that these features formed at the time of the mainshock, so we consider them to be possible surface coseismic ruptures. At SR3, an open crack has a minimum of 0.55 m of right-lateral horizontal offset (Fig. 10) along a N95° E fault. At SR4, a N100° E fault clearly displaces the edge of a small road (Fig. 10), very similar in character to the SR1 site, with a right-lateral horizontal displacement of about 0.42 m. The other possible surface rupture feature (SR5 in Fig. 7) occurred at the El Carmen school (Fig. 10). The main fault here runs east–west beneath the floor tiles, producing small displacements on each tile with a total minimum right-lateral horizontal offset of about 0.3 m. This feature was identified on photos taken soon after the earthquake.

Coseismic displacements decreased gradually to the east. Cracked pavement was common on the Pan-American highway, where it is along the fault trace. However, not all ground cracks along the Pan-American road were fault-related (see the Off-Fault Deformation Features section). All surface-rupture observations plotted in a distance along the fault-displacement (Fig. 11) show a gradual eastward decrease in the displacements along the fault resulting from variations along the surface rupture during the event. There is a general eastward decreasing of horizontal displacements that agrees with the seismological slip model of Kikuchi and Yamanaka, (2001). Westward decrease of slip from SR1 probably also occurred, however we did not find adequate places to measure it.

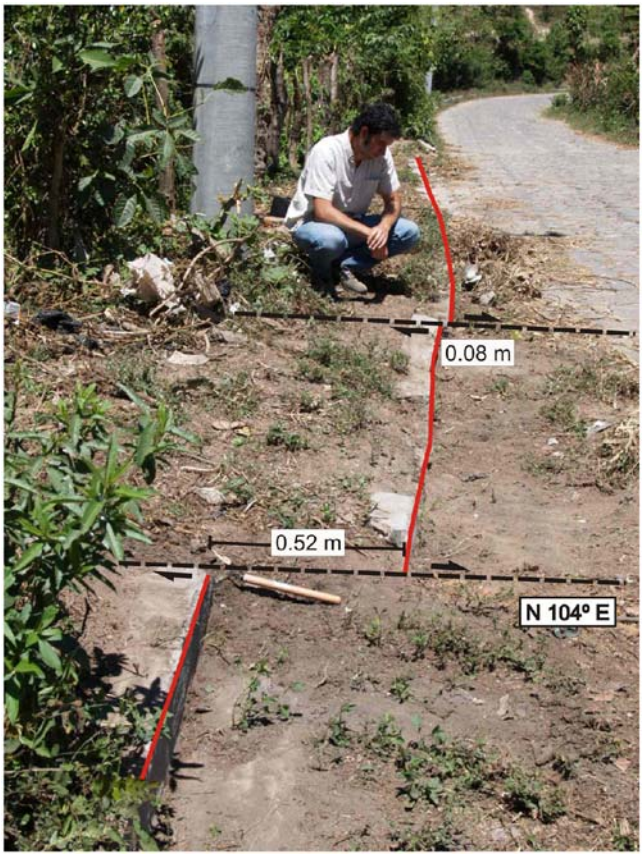


**Figure 8.** Surface rupture on the San Vicente segment of El Salvador fault zone. Two fault strands, which have a total of about 0.6 m of pure horizontal right-lateral displacement, occurred at this location (see SR1 in Fig. 7). The color version of this figure is available only in the electronic edition.

## Off-Fault Deformation Features

The principal and most destructive effect of the earthquake shaking were hundreds of landslides. Landslides and related geological effects of the earthquake occurred over an area covering about 2500 km$^2$ and were particularly abundant in zones underlain by thick deposits of poorly consolidated late Pleistocene and Holocene Tierra Blanca rhyolitic tephras and of ignimbrites (and reworked materials) that were erupted from the Ilopango caldera (Rose *et al.*, 1999).

Maps of the location of more than 40 landslides and rockfalls triggered by the earthquake (Fig. 12) compiled by García-Flórez, (2008) and Tsige *et al.* (2008). If we do not consider those landslides that occurred on the slopes of San Vicente Volcano and the Ilopango caldera, the spatial distribution of the remainder are confined to a narrow band of 25 km length, similar to the distribution of aftershocks (Fig. 2 and Fig. 12). The larger, more destructive landslides were located close to the main and secondary traces of the San Vicente segment of the ESFZ, where larger ground acceleration is expected.

Other off-fault ground-deformation features were abundant and in most cases were readily attributable to lateral spreading, landslides, ground cracking, and liquefaction. East–west trending fissures, en-echelon fractures along topographic highs (Fig. 13a), and some liquefaction occurred along the fault zone. Differential settlement and cracking of man-made fill resulted in minor-to-severe damage to structures, buildings, roads, and highways (Fig. 13b) throughout the region.

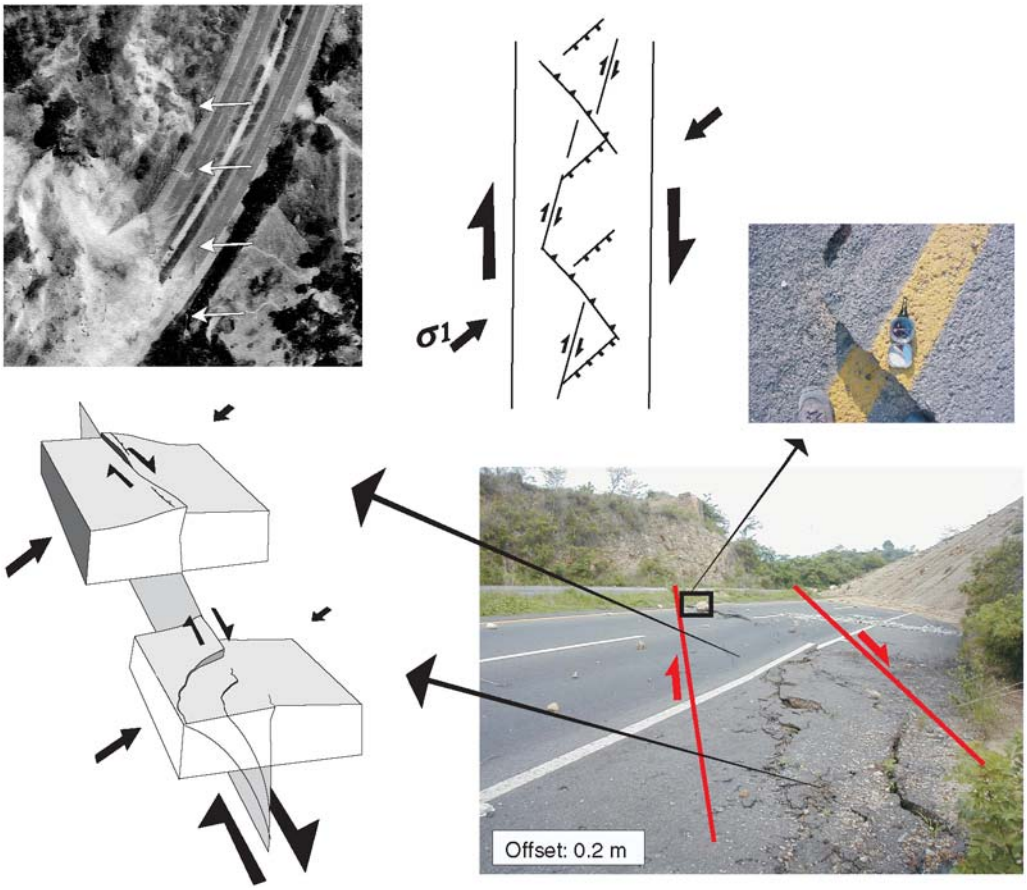


**Figure 9.** Coseismic surface rupture of the San Vicente segment of the ESFZ at the Pan-American Highway (SR2 on Figure 7). Photographs and sketches show the complex nature of the right-lateral strike-slip rupture. The color version of this figure is available only in the electronic edition.

## February 2001 Earthquake Source Parameters: Integration of Geological and Seismic Data

We use the distribution of seismicity, seismic moment release, active fault mapping, observations of on-fault and off-fault coseismic deformation, and slip distribution to define the seismic source parameters of the 13 February 2001 El Salvador earthquake. Our aim is to characterize the fault associated with the earthquake and, if possible, the fault rupture parameters (area and slip).

We conclude that the earthquake occurred on the El Salvador faults zone as shown by observations of coseismic surface rupture along an east–west active fault trace in the area of the 2001 mainshock/aftershock sequence. The spatial distribution of aftershocks (Fig. 2 and Fig. 3) and landslides (Fig. 12) also suggests that the rupture was on an east–west trending plane subparallel to the volcanic chain and to the ESFZ. Right-lateral horizontal displacement observed on surface ruptures and the general east–west-trending (Fig. 7), steeply south-dipping rupture plane derived from the aftershock sequence (Fig. 3) agree with the focal mechanism proposed by Buforn *et al.* (2001) for the 13 February earthquake.

The fault rupture length associated with the 13 February 2001 earthquake can be estimated from the analysis of the aftershock distribution, a map of the energy release, and the spatial distribution of on-fault and off-fault deformation features. The distribution of the aftershocks up to six months after the mainshock extends about 50 km along the San Vicente and Lempa segments, which is a larger area than the rupture length proposed by Kikuchi and Yamanaka (2001); their finite-source slip model covers only the San Vicente segment (21 km). A similar rupture length to the one from the finite-source slip model is suggested by the energy released map (Fig. 4) and the landslide distribution (about 25 km long, including the San Vicente segment and Ilopango Lake). Surface observations show clear surface faulting for at least 12 km (from site SR1 to La Curva landslide [Ls3]) along the San Vicente segment (Fig. 7).

Thus, we interpret the 13 February 2001 earthquake sequence to be the result of rupture of the San Vicente segment with a length of at least 12 km (surface-fault rupture) and possibly the full 21-km segment length. It is difficult to assess whether the rupture extended into the Ilopango caldera or whether it was arrested at the caldera margin. Our best


**Figure 10.** Surface ruptures on the San Vicente segment at locations SR3, SR4, and SR5. See Figure 7 for locations. The color version of this figure is available only in the electronic edition.

estimate of the rupture length, based on the mapped length of the San Vicente segment is approximately 21 km.

The seismic moment of the 2001 earthquake is in the range of $6.05–8.1 \times 10^{18}$ N m (Table 1). Using the fault parameters derived from geological observations, and geometric interpretation of the earthquake sequence, we can assess how well the assigned fault parameters compare with the energy release observed by using both the Aki and Richards (1980) equation linking seismic moment with crustal rigidity, fault area, and average fault plane displacement ($M_o = \mu ad$, where $\mu$ is rigidity of the crustal material involved in the rupture, usually $3 \times 10^{11}$ Nm; $a$ is the rupture area; and $d$ is average displacement) and from fault rupture scaling relations derived from historical earthquake data (e.g., Wells and Coppersmith, 1994).

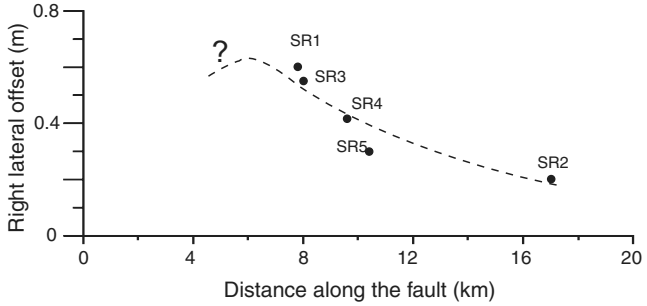


**Figure 11.** Displacement-distance plot of right-lateral strike-slip offset along the San Vicente segment. Origin of plot is the western end of the segment. Maximum displacement is observed in the central part of the segment.

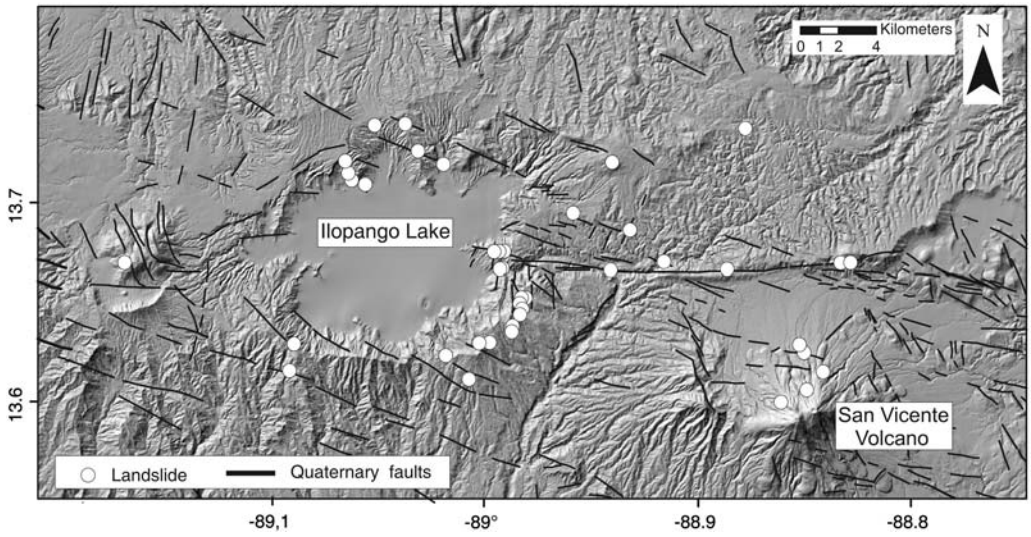


**Figure 12.** Distribution of landslides generated by the 13 February 2001 earthquake, showing the concentration around the steep caldera margin of Ilopango Lake, on the flanks of San Vicente volcano, and along the San Vicente segment of the ESFZ.

The seismological data suggest the mainshock ruptured at about 15 ± 2 km depth on a very steep fault (Table 1), and 95% of all the aftershocks are at or shallower than 15 km. The minimum rupture length in 2001 is 12 km based on the observed surface -rupture length, and the whole San Vicente segment is 21 km long. Thus considering the fault dips 75°, the fault area of the 2001 earthquake is at least 183 $km^2$ and more probably 326 $km^2$. This latter area implies full segment rupture, which is compatible with the region of the first few hours of aftershocks. Using the Aki and Richards (1980) equation with these parameters derives an average fault plane displacement of about 0.6 m for the full segment rupture. This compares well with the average surface slip of 0.42 m calculated from the five measurements of slip (Fig. 11) and with the finite-fault slip model of Kikuchi and Yamanaka (2001), which suggests about 0.5 m of slip may have occurred at the surface (Fig. 4, inset).

From the Wells and Coppersmith (1994) relations linking magnitude with average surface displacement and surface-rupture length (Table 1), we obtain an expected average surface displacement of 0.37 m for an $M_w$ 6.6 earthquake and a surface-rupture length of 19.3 km. These values are consistent with observed average surface displacement of 0.42 m and San Vicente segment length of 21 km.

## Stress Transfer in the 2001 Earthquake Sequence

From the previous seismotectonic analysis, we observe that the distribution of the aftershocks following the mainshock covers an area that is much longer than the fault plane

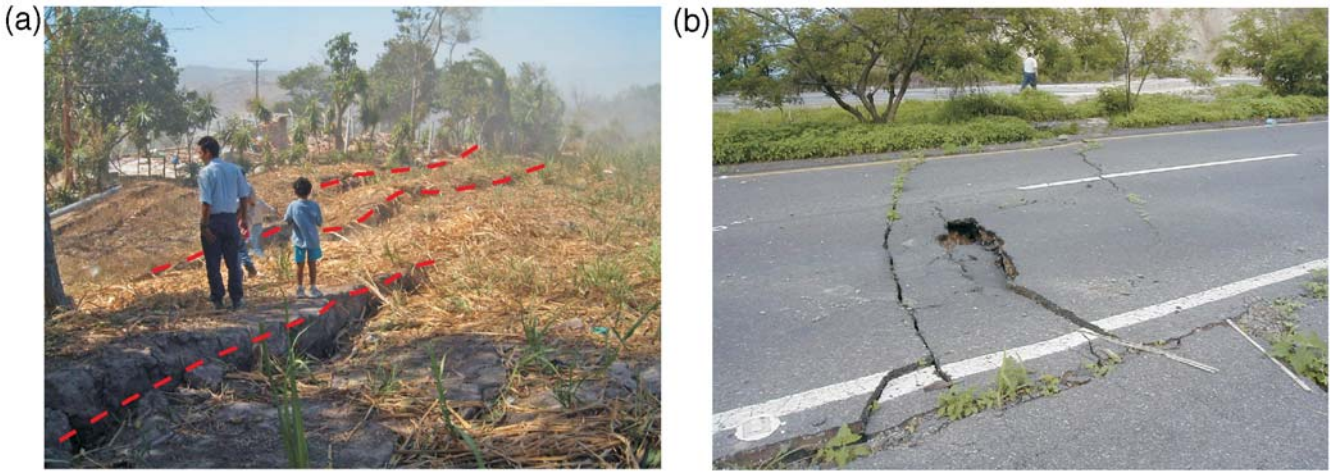


**Figure 13.** Off-fault secondary features produced by ground shaking that occurred during the 13 February 2001 earthquake along the San Vicente segment of the ESFZ. (a) En echelon fractures on a ridge interpreted as a result of topographic amplification of shaking. (b) Fractures across the Pan-American Highway produced by differential settlement. The color version of this figure is available only in the electronic edition.

Table 1
13 February 2001 Earthquake Parameters

| Harvard (CMT) | USGS (CMT) | Buforn *et al.*, 2001 Inversion *P* wave | MARN-SNET | Bommer *et al.*, 2002 | Wells and Coppersmith, 1994 Empirical Relations for *M* 6.6 Earthquakes | This Study |
|---|---|---|---|---|---|---|
| $M_o$ $8.1 \times 10^{18}$ N m | $M_o$ $6.2 \times 10^{18}$ N m | $M_o$ $6.05 \times 10^{18}$ N m | | $M_o$ $6.05 \times 10^{18}$ N m | AD = 0.37 m | AD = 0.42 m |
| $M_w$ 6.6 | $M_w$ 6.5 | $M_w$ 6.5 | $M_w$ 6.6 | | SRL = 19.3 km | SRL = 21 km |
| *Time:* 14:22:16.40 (UTC) | *Time:* 14:22:05.82 (UTC) | *Time:* 14:22:16 (UTC) | *Time:* 08:22 (UTC) | | RA = 370.4 $km^2$ | RA = 315 $km^2$ |
| | | | | | RLD = 33.4 km | |
| *Epicentral location:* Lat 13.98° N; Lon 88.97° W Depth: 15 km | *Epicentral location:* Lat 13.67° N; Lon 88.94° W Depth: 15 km | *Epicentral location:* Lat 13.60° N; Lon 88.96° W Depth: 14 km STF: 14S | *Epicentral location:* Lat 13.60° N; Lon 88.85° W Depth: 9 km | *Epicentral location:* Depth: 14 km Duration: 12 s | *Parameters derived from scaling relationships:* $M_w = 7.04 + 0.89 \log AD$; $M_w = 5.16 + 1.12 \log SRL$; $M_w = 3.98 + 1.02 \log RA$; $M_w = 4.33 + 1.49 \log RLD$, $M_w$ = earthquake magnitude AD = average displacement SRL = surface rupture length RA = rupture area RLD = subsurface rupture length | *Parameters derived from field data of this study and the seismic information, with the rupture of the San Vicente segment as source of the 13 Feb. 2001 El Salvador earthquake:* RL = rupture length |
| *p1:* STK, 276°; DP, 74°; slip: −175° | *p1:* STK, 96°; DP, 81°; slip: −178° | *p1:* STK, 90°; DP, 191°; slip: −180° | *Location:* Lat 13.621° N Long 88.856° W San Vicente | Strike slip. Fault plane subparallel to the subduction trench | *Location:* Lat 13.621° N Long 88.856° W San Vicente | |
| *p2:* STK, 7°; DP, 86°; slip, −16° | *p2:* STK, 6°; DP, 88°; slip, −9° | *p2:* STK, 90°; DP, 101° | | | El Salvador fault zone; strike-slip fault plane parallel to volcanic arc | |
| *Axis T, NYP* 1. (T) VAL = 8.50; PL = 14; AZM = 233 2. (N) VAL = −0.83; PL = 73; AZM = 22 3. (P) VAL = −7.66; PL = 8; AZM = 141 | *Axis T, NYP* 1. (T) VAL = 6.17; PL = 5; AZM = 51; 2. (N) VAL = −0.02; PL = 81; AZM = 173 3. (P) VAL = −6.14; PL = 7; AZM = 321 | | | | | |

$M_o$, moment magnitude; $M_w$, earthquake magnitude; p, plane; STK, strike; DP, dip; VAL, value; PL, plunge; AZM, azimuth; AD, average displacement; SRL, surface rupture length; RA, rupture area; LD, subsurface rupture length.

that produced the earthquake. This suggests that the seismic activity occurred in the Lempa area (triangles denoting epicenters in Fig. 3) and other surrounding areas could have been promoted by static stress transfer produced by the February 2001 mainshock. A high density of active faults surrounds the Ilopango–San Vicente segment and continues to the east of the principal displacement zone of the ESFZ towards the Lempa segment and the Berlin segment. The spatial coincidence of aftershock seismicity and active faults provides the perfect scenario to quantify static stress transfer to understand the influence of the 2001 event in the future seismic activity of the area. In order to test this, we modeled the static Coulomb stress change produced by the mainshock and the larger aftershock on fault planes with azimuth and dips as defined in the active fault map (Fig. 6) (see Table 2 for model parameters). We refer to the faults on which the stresses are exerted as "receiver faults."

The stress drop on a fault plane due to the occurrence of an earthquake produces an increase in effective shear stress in the area around the rupture area (Chinnery, 1963). This transfer of the static stress may explain the generation and location of aftershocks and other mainshocks at large distances from the fault, even at tens of kilometers, in those areas where the Coulomb failure stress (CFS) increases. This has been recognized in numerous works in different geodynamic frameworks (e.g., Jaume and Sykes, 1992; King *et al.*, 1994; Toda *et al.*, 1998). These studies have indicated that minor (~1 bar) changes in static stress can induce reactivation of nearby faults that are close to failure, producing aftershock activity and/or larger earthquakes. This phenomenon has been described as a triggering process (King *et al.*, 1994; Harris *et al.*, 1998).

We constructed models of stress transfer between source fault rupture and receiver faults for two rupture sources: the ruptures associated with the February mainshock ($M_w$ 6.6) and the larger aftershock in May ($M_w$ 5.8). The rupture geometry used for the mainshock ($M_w$ 6.6) is showed in Table 1. In the case of the $M_w$ 5.8 aftershock, we used a rupture area of 8 × 5 km with a top depth of 7 km and a N106°/85°N fault plane orientation, based on the aftershocks distribution and the fault mapping. The CFS-stress-change receiver faults were selected acknowledging the existence of four sets of active faults in the region (N86°/75°S right-lateral strike slip, N106°/85°N right-lateral strike slip, N140°/90° normal fault slip, and N165°/80°W normal fault slip).

Figure 14 shows CFS stress-change scenarios produced by rupture of the San Vicente fault segment for four different orientations of receiver faults. The models show that the 13 February 2001 strike-slip earthquake in the San Vicente segment increases the CFS to the east where most of the $M_w$ > 4.6 aftershocks occurred. The best correlation between areas of increased CFS and the actual hypocentral locations of aftershocks is obtained when the CFS calculations are performed for N165° receiver normal faults. The model suggests that stress changes associated with the mainshock of the February 2001 triggered secondary rupture and associated aftershocks, mainly on extensional northwest–southeast-oriented faults located in the Lempa segment. These secondary rupturing processes explain the large size of the aftershock zone.

## Implications for Seismic Hazard

Our conclusion that the 13 February 2001 $M_w$ 6.6 earthquake was associated with rupture of the ESFZ has important implications for seismic hazard in El Salvador. The earthquake occurred on a fault that has similar geomorphic expression to many other faults mapped within the volcanic arc. Therefore, we infer other fault traces are also likely responsible for repeated large earthquakes in the past.

In the period since the 2001 earthquake, the ongoing pattern of seismicity indicates static stress transfer is an important phenomenon in the temporal occurrence of seismicity, as is the correlation of large earthquakes in El Salvador with geological structure (Martínez-Díaz *et al.*, 2004). The change

Table 2
Parameters Used in Coulomb Failure Stress Models Generated by the Three Events Studied*

| | Plane | | | Center of Rupture | | | | |
|---|---|---|---|---|---|---|---|---|
| Event Date dd/mm/yyyy | Strike | Dip | Rake | Latitude (°N) | Longitude (°W) | $M_w$ | Depth to Top of Rupture, $D_T$ (km) | Rupture Area (km) |
| 13/02/2001 | 86° | 75° | −179° | 13.67 | −88.94 | 6.6 | 0 | 24.3 × 11.2 |
| 08/05/2001 | 286° | 85° | −179° | 13.29 | −89.39 | 5.8 | 7 | 8 × 5 |
| 13/01/2001† | 30° | 60° | −98° | 13.1 | −88.9 | 7.7 | 20 | 60 × 42 |

*The triggering effect is attributed to changes in Coulomb failure stress (CFS): $CFS = \tau_\beta - \mu(\sigma_\beta - p)$, where $\tau_\beta$ is the shear stress over the fault plane, $\sigma_\beta$ is the normal stress, $p$ is the fluid pressure, and $\mu$ is the frictional coefficient. For the seismic series of 2001 in El Salvador, we have estimated the change in the static Coulomb failure stress by the expression given in the equation: $\Delta CFS = \Delta\tau_\beta - \mu'\Delta\sigma_\beta$, where $\Delta\tau_\beta$ is considered positive in the sense of the slip fault, and $\Delta\sigma_\beta$ is also positive in compressional regime. $\mu$ is the apparent coefficient of friction and includes the effects of pore fluid, as well as the material properties of the fault zone (see Harris, 1998, for a more complete explanation of this parameter). Positive values for ΔCFS are interpreted as promoting faulting, while negative values inhibit slip. We have estimated the stress-change in an elastic half-space following the Okada (1992) method, taking $8 \times 10^5$ bars as the Young's modulus and 0.25 as the Poisson coefficient. The apparent friction coefficient is taken as 0.4, which is an acceptable value as proposed by Deng and Sykes (1997). The USGS program COULOMB 3.1 (see Data and Resources) was utilized to make the stress calculations. To estimate the source parameters, we used information from the geological mapping of active faults, the focal mechanisms from the USGS CMT catalog (see Data and Resources) and Buforn *et al.* (2001), and the spatial analysis of the aftershocks population.

†From Martínez-Díaz *et al.* (2004).

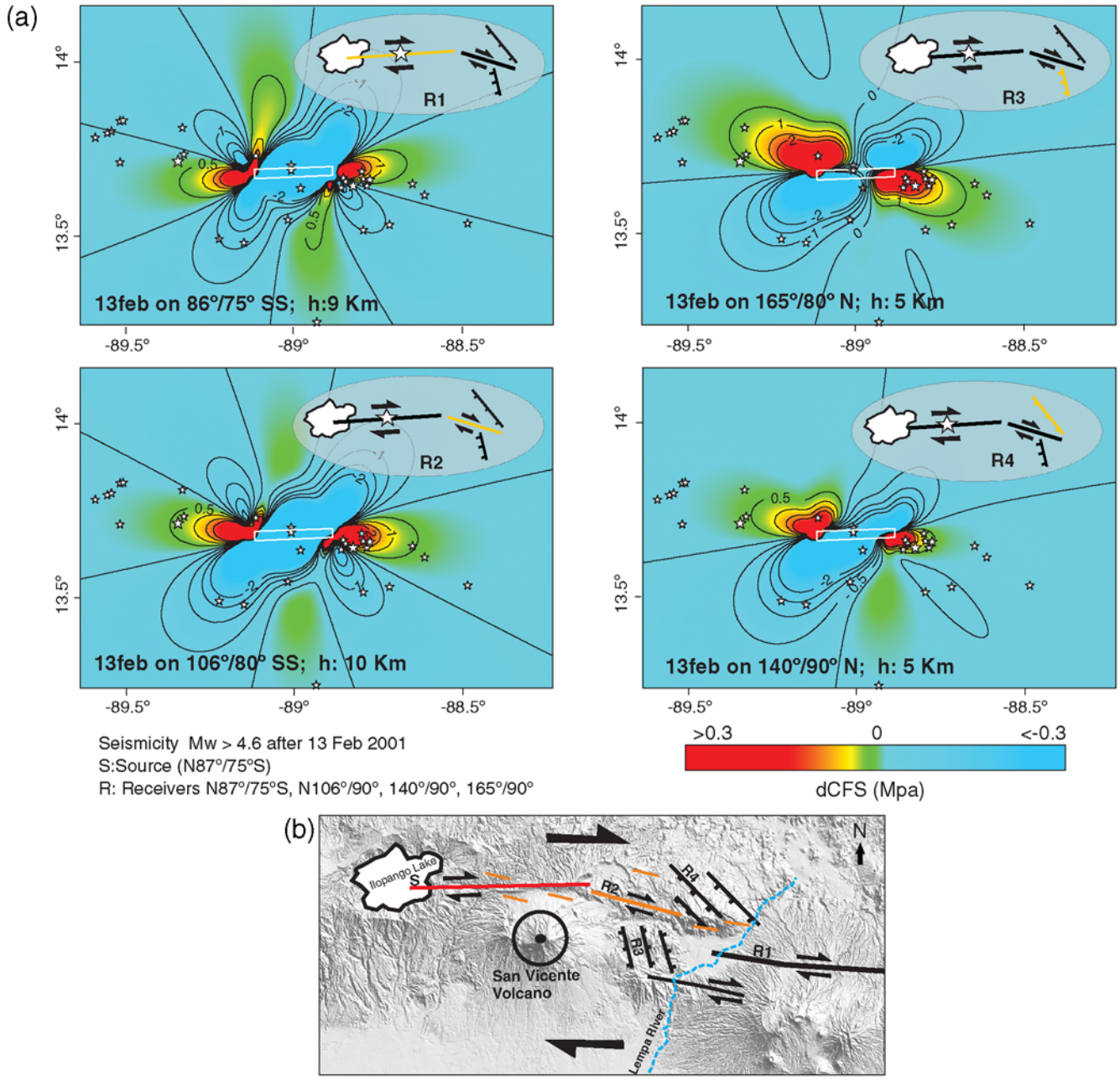


**Figure 14.** (a) Static Coulomb stress transfer models resulting from fault rupture in the 13 February 2001 earthquake on receiver faults having different orientations (receivers highlighted with light color in the insets). Dark areas (CFS > 0) show zones of predicted stress increase, while light areas (CFS < 0) represent zones of predicted stress decrease. Many of the larger aftershocks ($M_w$ > 4.6; stars) occur in the lobe of increased stress resulting from rupture of the San Vicente segment in the 13 February 2001 earthquake. N and SS refer to the kinematics of receiver faults in each model: normal fault and strike-slip faults respectively. White rectangles show the projections of the rupture areas modeled. (b) DTM with the sketch of the San Vicente segment source fault (S) and the receiver faults (R1–R4) of the Lempa segment. The color version of this figure is available only in the electronic edition.

in stress resulting from the 2001 mainshock on the east–west-striking San Vicente segment has loaded the Lempa and Berlin fault segments to the east (Fig. 14). Thus, the likelihood of rupture within a short period of time has increased in this area, and increased seismic activity could be expected. Indeed, most of the seismicity that has occurred since the 2001 sequence has occurred as swarms along the ESFZ and the volcanic arc in the positively stressed areas (Fig. 15). The activity triggered by the mainshock on the northwest–southeast faults close to the Lempa basin could have a potential effect on the stability of the Lempa and Berlin segments. This should be evaluated by future studies.

Three processes account for the recent seismicity: (1) volcanic seismicity related to the Ilopango caldera;

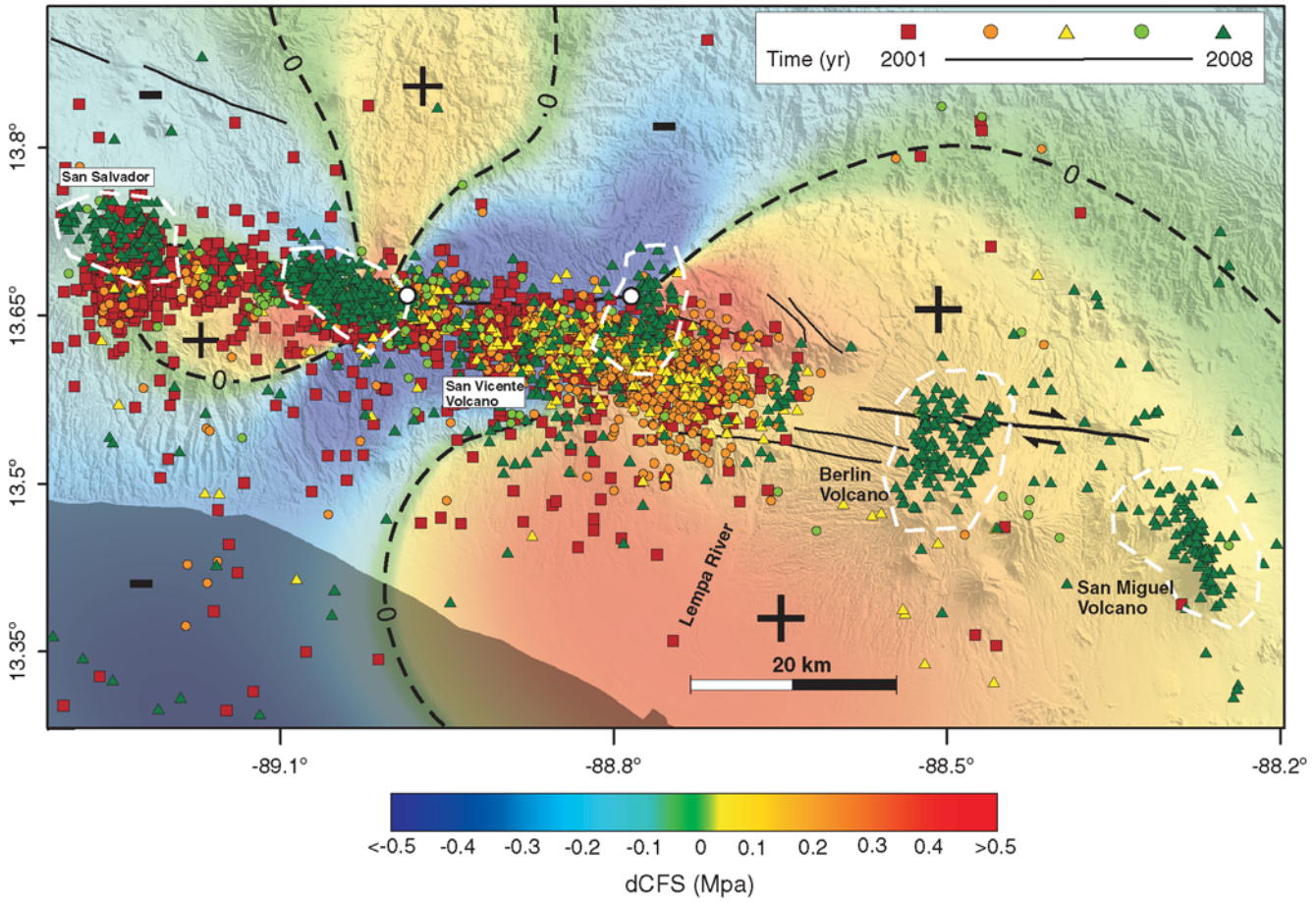


**Figure 15.** The association of the static Coulomb stress-change model resulting from rupture of the San Vicente segment in the 13 February 2001 earthquake and more recent shallow ($h$ < 15 km) seismicity between 2001 and 2008. Dark zones ($d$CFS > 0) show areas of predicted stress increase, while light zones ($d$CFS < 0) show areas of predicted stress decrease. Black lines, active fault traces in the area; white dashed lines enclose clusters or swarms of earthquake activity that generally occur within the lobes on increased static stress as a result of the 2001 fault rupture; white circles, the tips of the 13 February 2001 earthquake rupture. The color version of this figure is available only in the electronic edition.

(2) volcano–tectonic activity linked to inflation–deflation of the San Miguel volcano interacting with a north-northwest–south-southeast fault that crosses the volcanic edifice (Schiek *et al.*, 2008); and, (3) tectonic activity on the ESFZ. The most recent seismicity clusters (triangles denoting epicenters, Fig. 15) occurs in several clusters along the ESFZ (ellipses in Fig. 15). Some approximately coincide with the tips of the ruptures associated with the February $M_w$ 6.6 and the May $M_w$ 5.8 events.

The 13 February 2001 $M_w$ 6.6 strike-slip earthquake and probably most of the destructive ($M_w$ > 6.0) historical events that occurred along the Salvadorian volcanic arc with epicenters located very close to the fault result from rupture of various segments of the ESFZ. As observed in the 2001 earthquake, these earthquakes pose a major societal risk in El Salvador due to rapid population expansion in areas of strong earthquake shaking, steep topography, and major landslide susceptibility, exacerbated by deforestation and poorly planned urbanization. However, the hazard and risk are poorly quantified because little information exists on the past rupture history of the ESFZ and on any possible interaction between tectonic events on the ESFZ and volcanic activity. Recent palesoeismic studies (Canora *et al.*, 2008; Martínez-Díaz *et al.*, 2009) are attempting to document the past history of the ESFZ and rupture parameters (recurrence interval, elapsed time since the last rupture, and rupture size). One major question is whether multiple segments of the ESFZ can rupture together, resulting in an earthquake significantly larger than the $M_w$ 6.6 mainshock of the 2001 sequence. The answer to this question will have a large impact on the seismic hazard in large parts of El Salvador.

## Conclusions

The 13 February 2001 El Salvador earthquake was associated with rupture of the 21-km-long, 70°–85°S-dipping, right-lateral strike-slip San Vicente segment of the El Salvador fault zone. Surface rupture occurred along a preexisting but previously unrecognized fault trace. Retrospective identification of coseismic surface ruptures, together with

mapping of active fault traces of the ESFZ, analysis of focal mechanisms, and energy release in the 2001 sequence and mapping of the spatial distribution triggered landslides, provide a dataset with which to understand the context and hazard implications of the event. Coseismic surface ruptures associated with the 13 February 2001 earthquake have been identified at five locations along the fault trace, with a maximum strike-slip displacement of 0.6 m along the segment. The active fault map suggests the ESFZ consists of at least four geometric segments. The 2001 earthquake appears to have ruptured the entire the San Vicente segment, so the geometric segments may also define fault rupture segments.

Seismicity that has occurred following the 2001 sequence is highly correlated with arc volcanoes and with sections of the ESFZ that are in areas of increased static Coulomb stress changes resulting from the 2001 sequence, suggesting high levels of interaction between elements of the fault zone and the adjacent volcanic belt. Thus, the Lempa and Berlin fault segments located east of the 2001 rupture may have been brought closer to failure because of the 2001 sequence. Although few data exist concerning rupture and recurrence parameters on segments of the ESFZ, the widespread surface expression of faults in the Salvadorian landscape, which is largely of late Quaternary age, suggests youthful movement on the faults and indicates that the probability of future moderate earthquakes in El Salvador is high.

At $M_w$ 6.6, the 2001 earthquake was only a moderate-magnitude event, yet it caused tectonic rupture, ground shaking, landslides, and secondary ground deformation, as well as significant damage and numerous deaths and injuries. Thus, earthquake hazard and risk in the vicinity of the ESFZ, which straddles the city of San Salvador with a population of more than 2 million, is high because even moderate-magnitude events can cause major damage, deaths, and injuries in the region.

## Data and Resources

Seismic catalog utilized in this work was provided by the MARN–SNET local network (available at http://www.snet.gob.sv/ver/sismologia, last accessed October 2009) and the U.S. Geological Survey (USGS)–National Earthquake Information Center catalogs (available at http://earthquake.usgs.gov/regional/neic/, last accessed April 2009). Coulomb stress modelling was carried out using COULOMB 3 from the USGS. Focal mechanisms were extracted from the Global Centroid Moment Tensor Project database, formerly known as the Harvard CMT catalog (searched using www.globalcmt.org/CMTsearch.html, last accessed May 2009) and from http://earthquake.usgs.gov/earthquakes/eqarchives (last accessed May 2009). Some plots were made using the Generic Mapping Tools version 4.2.1 (www.soest.hawaii.edu/gmt; Wessel and Smith, 1998).

## Acknowledgments

This research was funded by the Spanish Ministerio de Educación y Ciencia. Project GEOTACTICA: Analysis of the active tectonics and volcano-tectonic interactions in the El Salvador using geological, geotechnical, and geophysical data (Ref. CGL2009-14405-C02-02). We are also grateful to Brian Sherrod and an anonymous reviewer for constructive review and comments that helped to improve this work. We are grateful to colleagues at SNET (Servicio Nacional de Estudios Territoriales): Manuel Díaz, Douglas Hernández, and Walter Hernández for their assistance in the field and for helping us find documents and photographs of the February 2001 earthquake damage. C. Canora acknowledges financial support for this publication provided by a predoctoral grant of the Universidad Complutense de Madrid, Spain. Funding for P. Villamor's contribution was provided by the New Zealand Foundation for Research, Science and Technology and GNS Science.

## References

Agostini, S., G. Corti, C. Doglioni, E. Carminati, F. Innocenti, S. Tonarini, P. Manetti, G. Di Vincenzo, and D. Montanari (2006). Tectonic and magmatic evolution of the active volcanic front in El Salvador: Insight into the Berlin and Ahuachapan geothermal areas, *Geothermics* **35,** 368–408.

Aki, K., and G. P. Richards (1980). *Quantitative Seismology: Theory and Methods*, Vol. **I and II**, W. H. Freeman, San Francisco, 948 pp.

Álvarez-Gómez, J. A., P. T. Meijer, J. J. Martínez-Díaz, and R. Capote (2008). Constraints from finite element modeling on the active tectonics of northern Central America and the Middle America Trench, *Tectonics* **27,** TC1008, doi 10.1029/2007TC002162.

Baum, R. L., A. J. Crone, D. Escobar, E. L. Harp, J. J. Major, M. Martinez, C. Pullinger, and M. E. Smith (2001). Assessment of landslide hazards resulting from the February 13, 2001, El Salvador earthquake, *USGS Open-File Report, on-line edition, 01-119*, available at http://pubs.usgs.gov/of/2001/ofr-01-0119/ (last accessed October 2009).

Benito, B., J. Cepeda, and J. J. Martínez-Díaz (2004). Analysis of the spatial and temporal distribution of the 2001 earthquakes, in *Natural hazards in El Salvador* W. I. Rose, J. J. Bommer, D. L. López, M. J. Carr, and J. J. Major (Editors), Geol. Soc. Am. Special Paper **375,** 339–356.

Bommer, J., B. Benito, M. Ciudad-Real, A. Lemoine, M. López-Menjivar, R. Madariaga, J. Mankelow, P. Mendez-Hasbun, W. Murphy, M. Nieto-Lovo, C. Rodríguez, and H. Rosa (2002). The El Salvador earthquakes of January and February 2001: Context, characteristics and implications for seismic risk, *Soil Dynam. Earthq. Eng.* **22,** 389–418.

Buforn, E., A. Lemoine, A. Udias, and R. Madariaga (2001). Mecanismo focal de los terremotos de El Salvador, in *Memorias 2nd Congreso Iberoamericano de Ingeniería Sísmica*, Madrid, Spain, 16–19 October 2001,J. M. Martínez-Guevara (Editor), 115–118.

Canora, C., J. J. Martínez-Díaz, P. Villamor, K. Berryman, R. Capote, J. A. Álvarez-Gómez, M. Bejar, M. Tsige, and C. Pullinger (2008). First paleoseismic studies on the El Salvador fault zone, *33rd International Geological Congress*, Oslo, Norway, 5–14 August 2008.

Correa-Mora, F., C. DeMets, D. Alvarado, H. L. Turner, G. Mattioli, D. Hernández, C. Pullinger, M. Rodriguez, and C. Tenorio (2009). GPS-derived coupling estimates for the Central America subduction zone and volcanic arc faults: El Salvador, Honduras and Nicaragua, *Geophys. J. Int.* **179,** no. 3 1279–1291.

Corti, G., E. Carminati, F. Mazzarini, and M. O. Garcia (2005). Active strike-slip faulting in El Salvador, Central America, *Geology* **33,** 989–992.

Chinnery, M. A. (1963). The stress changes that accompany strike-slip faulting, *Bull. Seismol. Soc. Am.* **53,** no. 5 921–932.

Das, S., and C. Henry (2003). Spatial relation between main earthquake slip and its aftershock distribution, *Rev. Geophys.* **41,** no. 3 1013.

Das, S., and C. Scholz (1981). Off-fault aftershock clusters caused by shear stress increase? *Bull. Seismol. Soc. Am.* **71,** 1669–1675.

DeMets, C. (2001). A new estimate for present-day Cocos–Caribbean plate motion: Implications for slip along the Central American volcanic arc, *Geophys. Res. Lett.* **28,** 4043–4046.

DeMets, C., R. G. Gordon, and D. F. Argus (2008). MOREL: A new estimate for geologically recent plate motions, *AGU Fall Meeting*, San Francisco, California, 15–19 December 2008.

Deng, J., and L. R. Sykes (1997). Evolution of the stress field in southern California and triggering of moderate-size earthquakes: A 200-year perspective, *J. Geophys. Res.* **102,** 9859–9886.

Dewey, J. W., R. A. White, and D. A. Hernández (2004). Seismicity and tectonic of El Salvador, in *Natural Hazards in El Salvador* W. I. Rose *et al.* (Editors), Geological Society of America Special Paper **375,** 363–378.

García-Florez, I.. (2008). Deslizamientos inducidos por terremotos: caso de El Salvador, *MSc Thesis*, Universidad Complutense de Madrid, 51_pp.

Guzmán-Speziale, M., and J. J. Meneses-Rocha (2000). The North America–Caribbean plates boundary west of the Motagua–Polochic fault system: A fault jog in southeastern Mexico, *J. S. Am. Earth Sci.* **13,** 459–468.

Guzmán-Speziale, M., W. D. Pennington, and T. Matumoto (1989). The triple junction of the North America, Cocos, and Caribbean plates: Seismicity and tectonics, *Tectonics* **8,** 981–997.

Harris, R. A. (1998). Introduction to special section: Stress triggers, stress shadows, and implications for seismic hazard, *J. Geophys. Res.* **103,** 347–358.

Isacks, B., and M. Baranzagi (1977). Geometry of Benioff zones: Lateral segmentation and downwards bending of the subducted lithosphere, in *Island Arcs, Deep Sea Trenches, and Back-Arc Basins*, Maurice Ewing Series, Vol. **I**, M. Talwani and W. C. Pitman (Editors), American Geophysical Union , Washington, D.C., 99–114.

Jibson, R. W., and A. J. Crone (2001). Observations and recommendations regarding landslide hazards related to the January 13, 2001 *M*-7.6 El Salvador Earthquake, *U.S. Geol. Surv. Open-File Report, on-line edition, 01-141*, available at http://pubs.usgs.gov/of/2001/ofr-01-0141/ (last accessed April 2009).

Jaume, S. C., and L. R. Sykes (1992). Changes in state of stress on the southern San Andreas fault resulting from the California earthquake sequence of April to June 1992, *Science* **258,** no. 5086 1325–1328.

Kanamori, H. (1977). The energy release in great earthquakes, *J. Geophys. Res.* **82,** no. 20 2981–2987.

Kikuchi, M., and Y. Yamanaka (2001). EIC Seismological Notes N° 99, Earthquake Research Institute, Tokyo, Japan, available through http://www.eri.u-tokyo.ac.jp/sanchu/Seismo_Note/index-e.html (last accessed April 2009).

King, G. C. P., R. S. Stein, and J. Lin (1994). Static stress changes and the triggering of earthquakes, *Bull. Seismol. Soc. Am.* **84,** 935–953.

Lyon-Caen, H., E. Barrier, C. Lasserre, A. Franco, I. Arzu, M. Chiquin, L. M. Chiquin, T. Duquesnoy, O. Flores, O. Galicia, J. Luna, E. Molina, O. Porras, J. Requena, V. Robles, J. Romero, and R. Wolf (2006). Kinematics of the North American–Caribbean-Cocos plates in Central America from new GPS measurements across the Polochic–Motagua fault system, *Geophys. Res. Lett.* **33,** L19309, doi 10.1029/2006GL027694.

Martínez-Díaz, J. J., J. A. Álvarez-Gómez, B. Benito, and D. Hernández (2004). Triggering of destructive earthquakes in El Salvador, *Geology* **32,** 65–68.

Martínez-Díaz, J. J., C. Canora, P. Villamor, R. Capote, J.A. Álvarez-Gómez, K. Berryman, M. Béjar, and M. Tsige (2009). Tectonic interpretation of the 13 February 2001, $M_w$ 6.6, El Salvador earthquake: New evidences of coseismic surface rupture and paleoseismic activity, *EGU General Assembly*, Vienna, Austria, 19–24 April 2009.

Okada, Y. (1992). Internal deformation due to shear and tensile faults in a half-space, *Bull. Seismol. Soc. Am.* **82,** no. 2 1018–1040.

Plafker, G. (1976). Tectonic aspects of the Guatemala earthquake of 4 February 1976, *Science* **193,** no. 4259 1201–1208.

Rose, W. I., F. M. Conway, C. R. Pullinger, A. Deino, and W. C. McIntosh (1999). An improved age framework for late Quaternary silicic eruptions in northern Central America, *Bull. Vulcanol.* **61,** 106–120.

Schiek, C. G., J. M. Hurtado, J. Aaron, A. Velasco, S. M. Buckley, B. Smith-Konter, and D. Escobar (2008). Determining volcanic deformation at San Miguel volcano, El Salvador by integrating radar interferometry and seismic analyses, Fall Meet. Suppl., Abstract U51A-0018, *Eos Trans. AGU*, **89,** no. 53.

Scholz, C. H. (1994). A reappraisal of large earthquake scaling, *Bull. Seismol. Soc. Am.* **84,** no. 1 215–218.

Selvaggi, G., B. Castello, and R. Azzara (1997). Spatial distribution of scalar seismic moment release in Italy (1983–1996): Seismotectonic implications for the Apennines, *Ann. Geophys.* **XL,** no. 6 1565–1578.

Sylvester, A. G. (1988). Strike-slip faults, *Geol. Soc. Am. Bull.* **100,** 1666–1703.

Toda, S., R. S. Stein, P. A. Reasenberg, and J. H. Dieterich (1998). Stress transferred by the $M_w = 6.5$ Kobe, Japan, shock: Effect on aftershocks and future earthquake probabilities, *J. Geophys. Res.* **103,** no. 24 543–565.

Tsige, M., I. García-Flórez, R. Capote, and R. M. Mateos (2008). Los grandes deslizamientos inducidos por los terremotos de El Salvador del 2001: Control litológico y estructural, *Geogaceta* **10**, 1567–5172.

Wessel, P., and W. H. F. Smith (1998). New, improved version of the Generic Mapping Tools Released, *EOS Trans. AGU* **79,** 579.

Wells, D. L., and K. J. Coppersmith (1994). New empirical relations among magnitude, rupture length, rupture width, rupture area and surface displacement, *Bull. Seismol. Soc. Am.* **84,** no. 4 974–1002.

White, R. A., and D. H. Harlow (1993). Destructive upper crustal earthquakes of Central America since 1900, *Bull. Seismol. Soc. Am.* **83,** 1115–1142.

White, R. A., D. H. Harlow, and S. Álvarez (1987). The San Salvador earthquake of October 10, 1986: Seismological aspects and other recent local seismicity, *Earthq. Spectra* **3,** 419–434.

Departamento de Geodinámica
Facultad de Ciencias Geológicas
Universidad Complutense de Madrid
Ciudad Universitaria
28040 Madrid, Spain
ccanora@geo.ucm.es
(C.C., J.J.M., R.C.)

GNS Science
Lower Hutt, New Zealand
P.Villamor@gns.cri.nz
(P.V., K.B.)

Instituto de Hidráulica Ambiental "IH Cantabria"
Universidad de Cantabria
E.T.S.I. Caminos, Canales y Puertos
Santander, Spain
(J.A..-G.)

LaGeo.S.A. de C.V.
Santa Tecla
La Libertad, El Salvador
(C.P.)

Manuscript received 11 December 2009